ISIJ International, Vol. 60 (2020), No. 5, pp. 971–978

Feasibility Investigation for Online Elemental Monitoring of Iron and Steel Manufacturing Processes using Laser-Induced Breakdown Spectroscopy

Zhenzhen WANG,[1,2] Yoshihiro DEGUCHI,[1,2]* Fangjung SHIOU,[3] Seiya TANAKA,[2] Minchao CUI,[2,4] Kai RONG[1] and Junjie YAN[1,2]

1) State Key Laboratory of Multiphase Flow in Power Engineering, Xi'an Jiaotong University, No. 28, Xianning West Road, Xi'an, 710049 China.
2) Graduate School of Advanced Technology and Science, Tokushima University, 2-1, Minamijyosanjima, Tokushima, 770-8506 Japan.
3) Department of Mechanical Engineering, National Taiwan University of Science and Technology, No. 43, Sec.4, Keelung Rd., Taipei, 10607 Taiwan.
4) Key Laboratory of High Performance Manufacturing for Aero Engine (MIIT), Northwestern Polytechnical University, Xi'an 710072 China.

(*Received on May 22, 2019; accepted on October 23, 2019; J-STAGE Advance published date: December 28, 2019*)

The metallurgical industries are very important for social development. In order to improve the metallurgical techniques and quality of products, the real-time analysis and monitoring of iron and steel manufacturing processes are very significant. Laser-induced breakdown spectroscopy (LIBS) has been studied and applied for the contents measurement of iron and steel. In this paper, the remote open-path LIBS measurement was studied under different sample temperature, lens to target distance (LTD), sample angle conditions to clarify its online measurement features. The 3D profile measurement system of parallel laser beam fringes projection was also developed to measure the sample profile at different sample temperature. The measurement results demonstrated the robustness of remote open-path LIBS system and 3D profile measurement system. However, the correction is necessary to enhance the detection ability of LIBS online measurement. In order to improve the precision and accuracy of real-time elemental measurement, an innovative co-axial laser beam measurement system combining LIBS and 3D profile techniques is proposed to automatically adjust the focus unit and measure the sample components. The further study of this promising method will be developed for online application of iron and steel manufacturing processes.

KEY WORDS: laser-induced breakdown spectroscopy; 3D profile; remote measurement; iron and steel manufacturing processes.

1. Introduction

Metallurgical industry is the resource and energy intensive industries. There are several classifications of metallurgical industry to different purpose. The iron and steel are the important raw materials of industrial production, such as transportation, infrastructure, power plants and so on. The development of metallurgical techniques is very essential for iron and steel manufacturing processes. Meanwhile, the reasonable production processes and equipment parameters are beneficial to quality assurance of the products, as well as energy saving and environmental protection, to improve the efficiency of entire production processes. Therefore, the real-time analysis and monitoring of iron and steel manufacturing processes are very significant.[1)]

Various measurement approaches, such as biological methods, chemical methods, optical methods, *etc.*, have been developed for contents measurement, temperature measurement, inspection and so on according to various applications.[2–4)] X-ray absorption fine structures (XAFS) yielded by X-ray fluorescence (XRF) is a useful tool to clarify the chemical states and the local structures of specific elements in steel. The quantitatively of the XRF-yield XAFS for trace elements in steel was investigated with ppm range to analysis the chemical state and local crystal structure.[5)] Atomic spectrometry is sensitive for metal and semimetal elements. The chromatographic separation procedure was studied for the on-line and off-line modes of inductive coupled plasma-atomic emission spectroscopy (ICP-AES) and inductive coupled plasma-mass spectrometry (ICP-MS) analyses of high-purity iron and low alloyed steels.[6)] The atomic spectrometry with the electrothermal vaporisation (ETV) can determine not only metal elements but also nonmetal elements at low concentrations. The tungsten boat furnace (TBF) ICP-MS and TBF-ICP-AES was investigated to

* Corresponding author: E-mail: ydeguchi@tokushima-u.ac.jp
DOI: https://doi.org/10.2355/isijinternational.ISIJINT-2019-317

determine the volatile boric acid and total boron according to different vaporisation properties of boron compounds.[7] Due to the detection limit level and complex sample preparation procedures, these methods present certain restrictions for the real-time monitoring of iron and steel manufacturing processes. Laser-induced breakdown spectroscopy (LIBS) as an analytical detection technique based on atomic emission spectroscopy has attracted a great attention in various industries because of the non-contact, fast response and multi-dimensional features as the qualitative and quantitative analytical detection technique.[8–13] LIBS has been widely applied in the metallurgy field to demonstrate the practicability for process analysis and control factors monitoring.[14,15] During the iron and steel manufacturing processes, there are various types of materials including solid phase, liquid phase and gas phase, such as raw materials, smelting processes, products and slags, heavy metals in flue gas. LIBS can be applied throughout the whole processes due to the features of LIBS technique.

The environment near the production line usually is much worse than that in laboratory due to its high temperature, smoke dust and vibration conditions. In order to realize the online measurement and protect optical probes, the developed LIBS technique presented its potential for the remote and online analysis. The optical fiber cable was employed to transmit the plasma emission signals.[16,17] The double-pulse LIBS with a Cassegrain telescope was developed to monitor the liquid steel contents.[18] There are various researches demonstrated the feasibility of a remote open-path LIBS system for practical applications.[19–22] However, the improvement approaches of measurement accuracy for remote LIBS should also be extensively studied. One of the improvement approaches is the autofocus for LIBS, especially for remote measurement system. The laser beam focus of LIBS is one of the most important factors when applying LIBS for the iron and steel manufacturing processes with the change of target profile. 3D profile information of target is necessary to locate the focused laser beam. Therefore, 3D profile measurement technique becomes one of the possible solutions for LIBS practical applications. The non-contact laser assisted measurement system equipment is the dominant tool used for engineering measurement applications with the features of high measuring speed, lack of contact force and no probe radius compensation calculation, *etc.*[23–27]

If a 3D profile measurement system can be integrated with a LIBS, the measured 3D profile information of the target can be used for the real-time positioning of a focused laser beam in a LIBS system. According to the 3D profile measurement results, the control system can automatically adjust the laser, focus point and irradiation position for LIBS measurement. The measurement results of LIBS can be an indicator for the control of iron and steel manufacturing processes. **Figure 1** illustrates the schematic diagram of measurement control system for typical iron and steel manufacturing processes. In order to integrate and improve the performance of developed non-contact measurement system using advanced laser technologies for the application of several industries such as iron and steel manufacturing processes, this paper focuses on the measurement characteristics of remote open-path LIBS measurement and 3D profile measurement. The innovative co-axial laser beam measurement system combining LIBS and 3D profile techniques is also proposed in this study.

2. Theory

In LIBS processes, a laser beam is focused into a small area to produce hot plasma. The material contained in plasma is atomized and the light corresponding to a unique wavelength of each element is emitted from excited atoms in plasma. The measured elements can be qualitatively and quantitatively determined according to spectral wavelength and signal emission intensity. Despite the complex laser-induced plasma processes, the emission intensity from the atomized species can be calculated by following equation with uniform plasma temperature assumption.[10]

$$I_i = n_i K_{i,j} g_{i,j} \exp\left(-\frac{E_{i,j}}{kT}\right) \quad \text{..... (1)}$$

Here, I_i is the emission intensity of species i. n_i is the concentration of species i. $K_{i,j}$ is a variable that includes the Einstein A coefficient from the upper energy level j. $g_{i,j}$ is the statistical weight of species i at the upper energy level j. $E_{i,j}$ is the upper level energy of species i. k is the Boltzmann constant and T is the plasma temperature.

3D profile measurement technique was also employed in

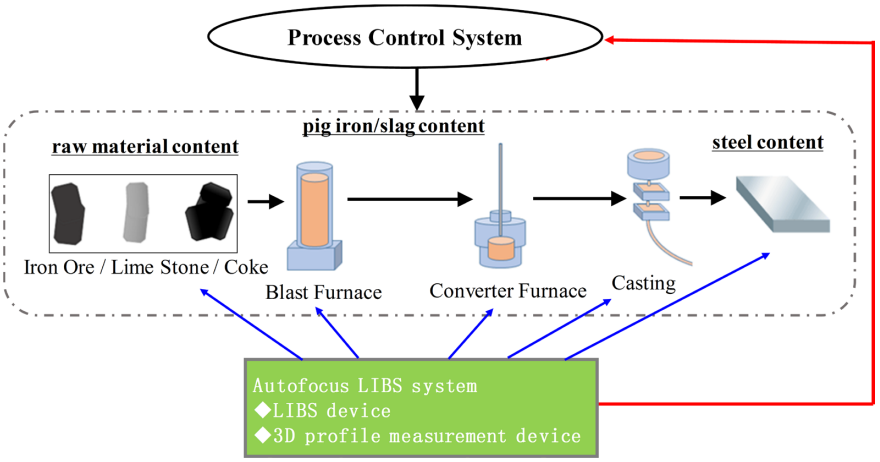

Fig. 1. Schematic diagram of measurement control system for typical iron and steel manufacturing processes. (Online version in color.)

this study. 3D laser imaging processes can be briefly summarized as follow. The laser beam focuses on the measured object. One or two CCD cameras are employed to acquire the line laser image on the object surface. 2D profile data can be calculated when extracting the line laser from image. By scanning the surface of measured object, 3D profile data are obtained.[28)]

3. Experiment

In order to integrate and improve the performance of non-contact measurement system using advanced laser technologies for industrial applications, the developed measurement systems of LIBS and 3D profile measurement are presented respectively.

3.1. LIBS Experimental System

Figure 2 illustrates the experimental setup of the remote open-path LIBS configuration consisting of a laser, digital delay generator, optical fiber, spectrometer, ICCD (Intensified Charge Coupled Device) camera and auxiliary equipment. A Q-switched Nd:YAG laser (LOTIS TII, LS-2134UTF, 5–8 ns, 10 Hz, beam diameter: 6 mm) operating at 1 064 nm was employed to induce plasma. A set of optical path adjustment system[29)] was employed to set the remote distances of 3.9 m and 1.2 m. The plasma emission signal was transmitted by the optical fiber and splitted by a spectrometer (SOL, NP-250-2M) with a holographic grating of 3 600 l/mm. An ICCD camera (Andor, iStar DH334T-18U-03) was employed to detect the emission intensity of plasma. The spectra resolution was 0.0073 nm/pixel and the spectra range was 400 nm-408 nm. The delay time of ICCD was triggered by the Q-switched signal of laser through a digital delay generator (Stanford Research Systems, Model DG645). An accumulation of pulses was used to reduce the influence of pulse energy fluctuation. A repetition of 5 times was used to avoid the non-uniform effect of samples under each experimental condition. The measured sample was placed in a muffle furnace with a through-hole in the front door on the adjustable movement stage.

Different standard steel samples employed in the experiments were provided by Zhengzhou Research Institution of Mechanical Engineering (ZRIME). The compositions were determined by various spectroscopy and chemical analysis methods for different elements, such as atomic absorption spectroscopy (AAS), inductively coupled plasma (ICP), potassium periodate spectrophotometric method, sodium arsenite - sodium nitrite volumetric method, and so on. The contents of manganese (Mn) element in different standard steel samples are listed in **Table 1**. Iron (Fe) contents listed in Table 1 were calculated by subtracting the provided other

Table 1. Manganese (Mn) and iron (Fe) contents of standard steel samples.

No.	Sample	Content (%)	
		Mn	Fe*
1	YSBS451073-13	0.032	99.742
2	YSBS37207-15	0.440	98.755
3	YSBS37209-15	0.472	98.479
4	YSBS37211-15	0.752	97.720
5	YSBS37212-15	0.778	97.575
6	YSBS37215-15	0.842	96.996
7	YSBS37217-15	0.957	96.348
8	YSBS37223-15	1.12	97.519
9	YSBS37218-15	1.23	97.423
10	YSBS37219-15	1.36	97.007

Symbol '*' means the value was calculated by subtracting the provided other major elements.

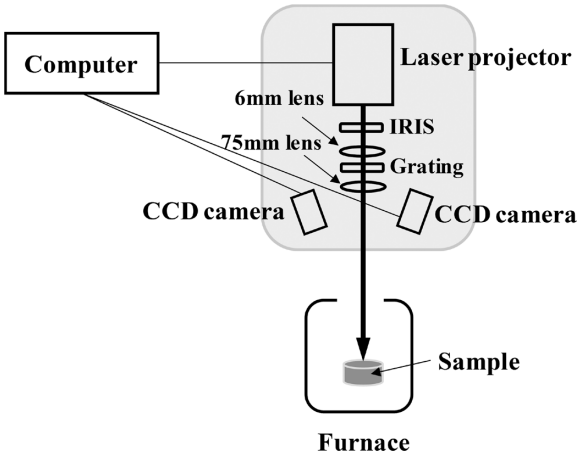

Fig. 3. Schematic illustration of parallel laser beam fringes projection system.

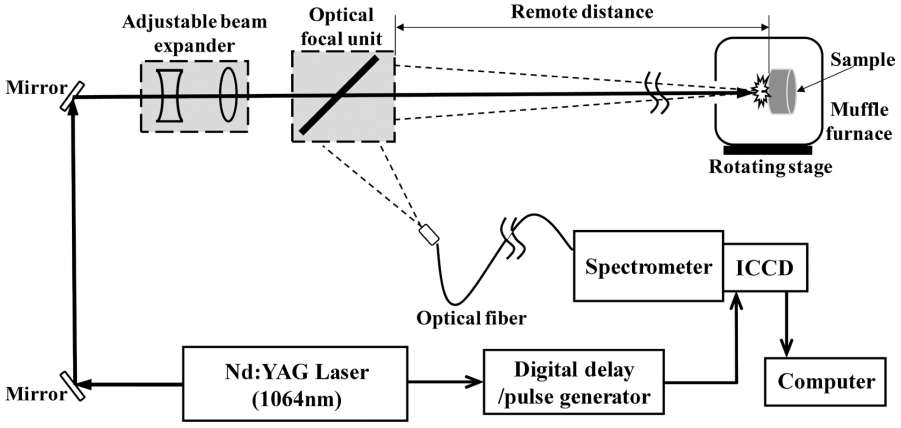

Fig. 2. Schematic diagram of remote open-path LIBS configuration.

major elements.

3.2. 3D Profile Measurement System

In order to improve the performance of fringes projection in-situ non-contact 3D profile measurement to adjust the focus point according to different measured samples, a new parallel laser beam fringes projection system integrating with the heating furnace was designed as shown in **Fig. 3**. The experimental system consists of laser fringes projection system, heating furnace and PC based software. The green light laser projector (LBS-532 Pattern Projecting Laser, 200 Hz, beam diameter: 4 mm) was employed as the light source, which was adjusted by a series of optics. Two CCD cameras (Image Source, DMK-23U618) with the resolution of 640×480 pixel were utilized to detect the profile signals. The laser fringes projection system was integrated in a portable box. The heated slag as the measured sample in furnace was about 1.2 m far from the dual-CCD camera system for remote measurement. The temperature of furnace was up to 1 000°C.

4. Results and Discussion

4.1. Remote Open-path LIBS Measurement

In order to demonstrate the feasibility of this remote open-path LIBS system, different steel samples were measured at the focus point with the lens to target distance (LTD) of 3.9 m. **Figure 4** shows the remote LIBS measurement results at room temperature and focus point. The measured spectra of sample No. 10 with 1.36%Mn in LTD of 3.9 m are shown in Fig. 4(a). Several emission lines of Fe and Mn elements can be clearly distinguished from the measured spectra with the resolution of 0.0073 nm/pixel. The wavelength and its parameters of measured emission spectra listed elsewhere[27] can be checked from the NIST (National Institute of Standards and Technology) database. This remote open-path LIBS measurement system was applicable for real-time elemental monitoring. Different steel samples were also measured using the remote LIBS system. The emission intensities of Mn I at 404.136 nm and Fe I at 400.524 nm were discussed in this study when considering Mn as the target element and Fe as the main element in steel samples. Figure 4(b) shows Mn/Fe concentration ratio dependence of $I_{\text{Mn-404.136 nm}}/I_{\text{Fe-400.524 nm}}$, which presents the good linearity with $R^2=0.9782$. It means that the credible results can be achieved using this remote LIBS measurement system.

4.2. Analysis of Effect Factors for Remote LIBS Measurement

In the real-time measurement of iron and steel manufacturing processes, there are various effect factors for the accurately quantitative LIBS analysis. Therefore, several effect factors, such as sample temperature, LTD and sample angle, were discussed for LIBS measurement.

4.2.1. Sample Temperature Effect

The physical processes involved in the generation and evolution of plasma can be effected by the sample temperature, which reveals a significant influence on laser-induced plasma signal. Sample No.10 with 1.36%Mn was measured under different sample temperature conditions in LTD of 3.9 m. **Figure 5** shows the measured spectra at sample temperature of room, 300°C, 500°C, 700°C. The emission intensity increased when increasing the sample temperature. In the laser-induced plasma processes, the laser energy is first absorbed by sample for ablation and vaporization. Under

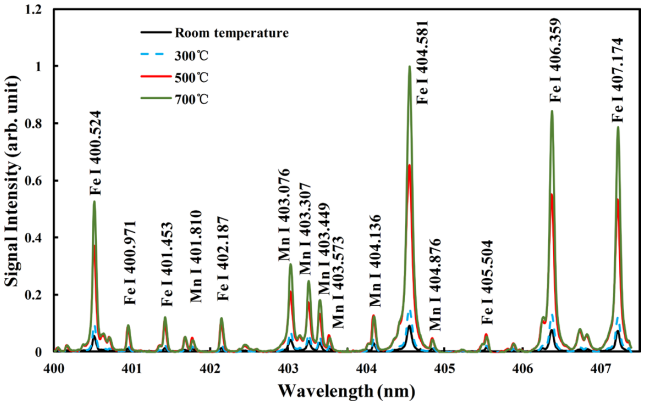

Fig. 5. Sample temperature effect on the measurement results in LTD of 3.9 m. Conditions: sample: No. 10 (1.36%Mn); laser power: 80 mJ/p; delay time: 500 ns; gate width: 1 000 ns; accumulation: 100; focus length: 3.9 m. (Online version in color.)

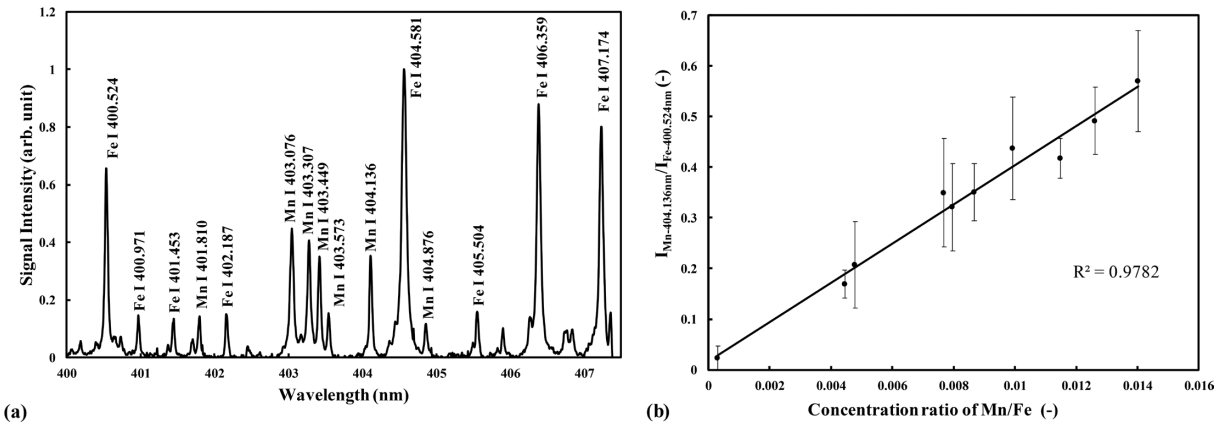

Fig. 4. Remote LIBS measurement result of different steel samples at focus point. Conditions: sample: 10 samples; laser power: 80 mJ/p; delay time: 500 ns; gate width: 1 000 ns; accumulation: 100; focus length: 3.9 m. LTD=3.9 m. (a) Measurement spectra of sample No. 10. (b) Mn/Fe concentration ratio dependence of I_{Mn}/I_{Fe} at focus point.

the same LIBS experimental conditions, when increasing the sample temperature, the laser energy for sample ablation and vaporization becomes lower and more laser energy can be used for plasma evolution processes to enhance the plasma emission intensity. The ablation and vaporization of sample also increase causing the increase of plasma emission intensity. Consequently, the emission intensity of measured spectra at higher sample temperature is higher than that at lower sample temperature.

The delay time dependence of signal intensities and the LTD effect on signal intensities at different sample temperature were studied and discussed to verify the sample temperature effect in detail.[29] In order to improve the accuracy of quantitative analysis, the calibration curves were established at different sample temperature taking Mn in the steel samples as example. The linearity and slope of calibration curves varied at different temperature. These results demonstrated that LIBS quantitative analysis should consider the sample temperature influence. There are several other approaches to improve the accuracy of quantitative analysis, such as correction factor of sample temperature, improvement of plasma stability to reduce sample temperature effect.[30,31]

4.2.2. Lens to Target Distance (LTD) Effect

Sample No. 10 with 1.36%Mn was measured in different LTD that is distance from target to the focus lens to investigate the LTD influence at room temperature. **Figure 6** shows the measured spectra at different LTDs of 3.5 m, 3.7 m, 3.9 m and 4.1 m. The emission lines of Fe and Mn were distinguished clearly from the measured spectra. The emission intensity in LTD of 3.9 m was the highest one, which was the focus length of 3.9 m. When increasing or decreasing LTD, the emission intensity decreased. At the focus point, the energy density of laser beam was highest. The results demonstrated the feasibility of remote open-path LIBS system in wide LTD range. However, the signal became very weak when the deviation between LTD and focus length was larger.

The different remote distances were employed to clarify the LTD effect for remote LIBS measurement. When the focus length was 1.2 m, the LTD effect was also studied. **Figure 7**(a) shows the measured spectra in different LTDs of 0.8 m, 1.0 m, 1.2 m and 1.4 m. The emission intensity decreased when LTD was not the focus length. The LTD dependences of Fe I at 400.524 nm and Mn I at 404.136 nm signal intensities were presented in Fig. 7(b). The signal intensities increased first and then decreased when increasing LTDs from 0.8 m to 1.5 m. The maximum signal intensities were obtained at the focus length, that is LTD of 1.2 m, due to the higher efficiency of laser ablation and vaporization for measured samples with the highest energy density of laser beam.

4.2.3. Sample Angle Effect

In the remote measurement, if the measured samples are tilted, the measured results can also be effected even if at the focus point. Sample No. 10 with 1.36%Mn was measured for different sample angles in LTD of 1.2 m at room temperature. The measured samples for LIBS here were the regular solid samples. The measured surface of sample was perpendicular to the laser beam direction. The measured sample was rotated based on this position of sample surface to discuss the sample angle effect. **Figure 8**(a) shows the measured spectra in different sample angles of 0°, 15°, 30° and 75°. When increasing the sample angle which means the sample surface was far away from the vertical direction of laser beam, the signal intensity decreased. The reason is

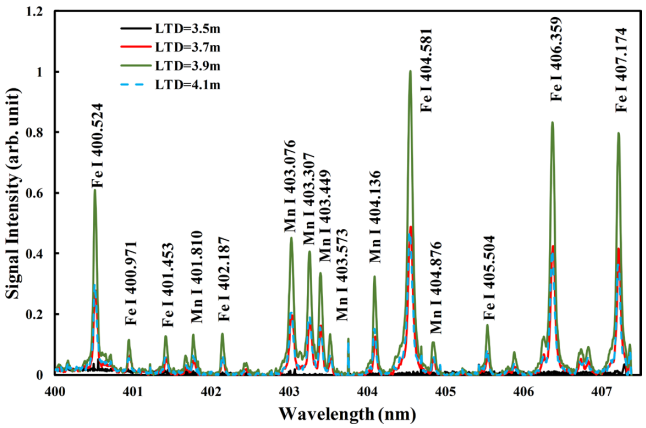

Fig. 6. LTD effect on the measurement results of long focus length spectra at room temperature. Conditions: sample: No. 10 (1.36%Mn); laser power: 80 mJ/p; delay time: 500 ns; gate width: 1 000 ns; accumulation: 100; focus length: 3.9 m. (Online version in color.)

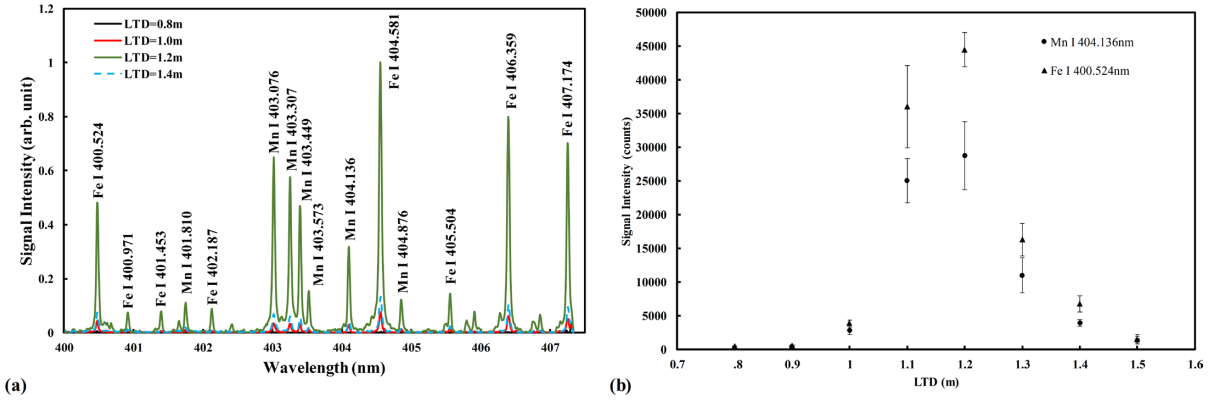

Fig. 7. LTD effect on the measurement results of short focus length spectra at room temperature. Conditions: sample: No. 10 (1.36%Mn); laser power: 50 mJ/p; delay time: 6 000 ns; gate width: 1 000 ns; accumulation: 50; focus length: 1.2 m. (a) Measured spectra in different LTD. (b) LTD dependence of signal intensity. (Online version in color.)

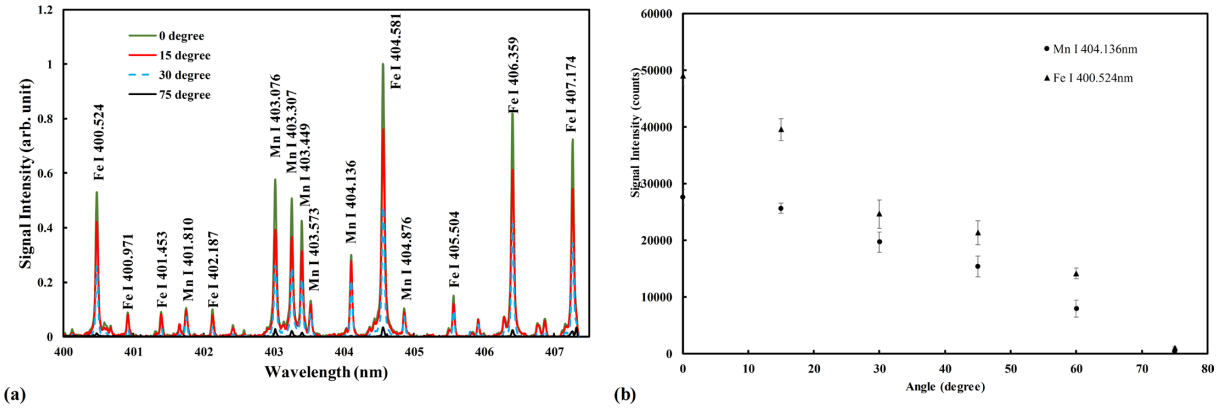

Fig. 8. Sample angle effect on the measurement results in LTD of 1.2 m at room temperature. Conditions: sample: No. 10 (1.36%Mn); laser power: 50 mJ/p; delay time: 7 000 ns; gate width: 1 000 ns; accumulation: 50; focus lens: 1.2 m. (a) Measured spectra in different sample angle. (b) Sample angle dependence of signal intensity. (Online version in color.)

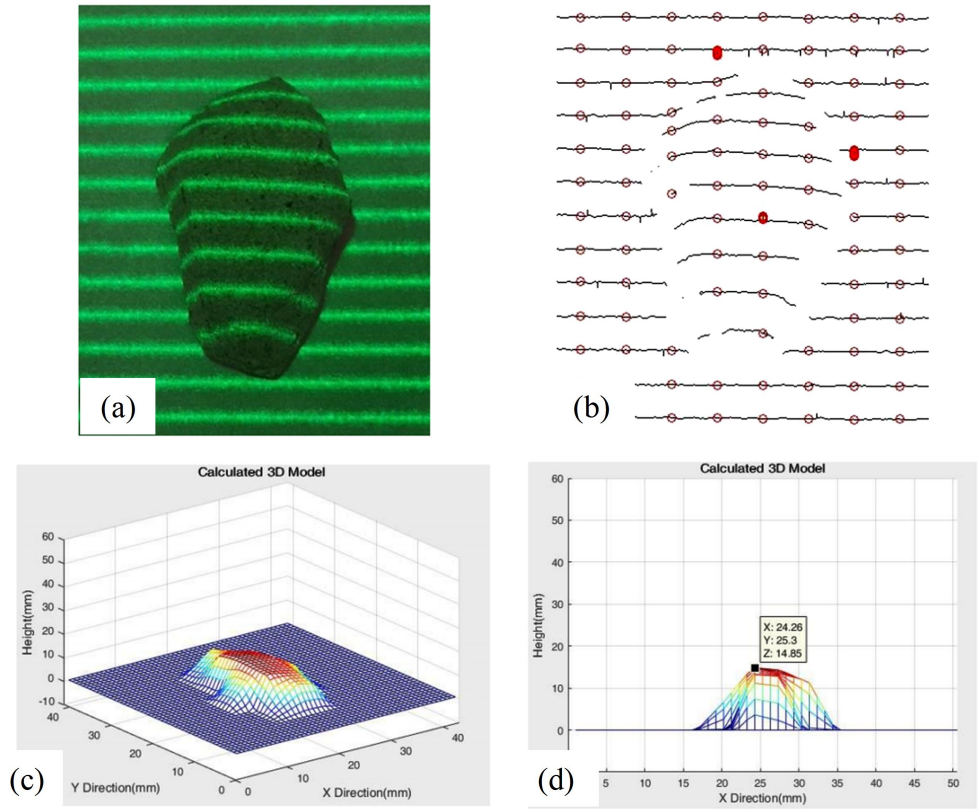

Fig. 9. Reconstructed profile at room temperature. (a) Laser irradiation. (b) Linearization. (c) 3D reconstruction. (d) Measured height of sample. (Online version in color.)

that the energy density of laser beam became lower at the measured point when the angle between the laser beam and sample surface increased. The sample angle dependences of Fe I at 400.524 nm and Mn I at 404.136 nm signal intensities were illustrated in Fig. 8(b). The signal intensities decreased when the sample angle increased. It can be seen from Fig. 8(b), If the sample angle increased over 45°, the signal intensity decreased obviously even if in LTD of 1.2 m.

According to these measured results in different LTDs and sample angles, it demonstrated the robustness of remote open-path LIBS system on LTD and sample angle. However, in order to improve the detection ability of this remote open-path LIBS system, the correction is very necessary for online measurement. The LTD should be adjusted to the focus length at the highest energy density based on the actual distance.

4.3. 3D Profile Measurement Result

The remote LIBS system can be applied for the online measurement. According to the plasma generation conditions, the laser focus is one of essential conditions to induce plasma, especially for the remote LIBS measurement. In order to adjust the focus point according to different measured samples for the improvement of quantitative analysis, 3D laser profile measurement technique was employed in this study.

The 3D profile measurement system with remote distance

of 1.2 m was developed as shown in Fig. 3. In order to verify the system feasibility, one sample of regular semi-ball was employed to detect its half 3D profile. It demonstrated the feasibility for 3D profile and dimension information. After the verification of measurement system, the irregular slag sample was measured at different temperature using this experimental system. **Figure 9** shows the image acquisition of slag sample at room temperature. 3D profile of measured slag was reconstructed using the fringes projection. The measured results were compared with that using coordinate measuring machine (Mitutoyo Crysta-APEZ C544) with the accuracy of 1.9 μm. The averaged relative error in three

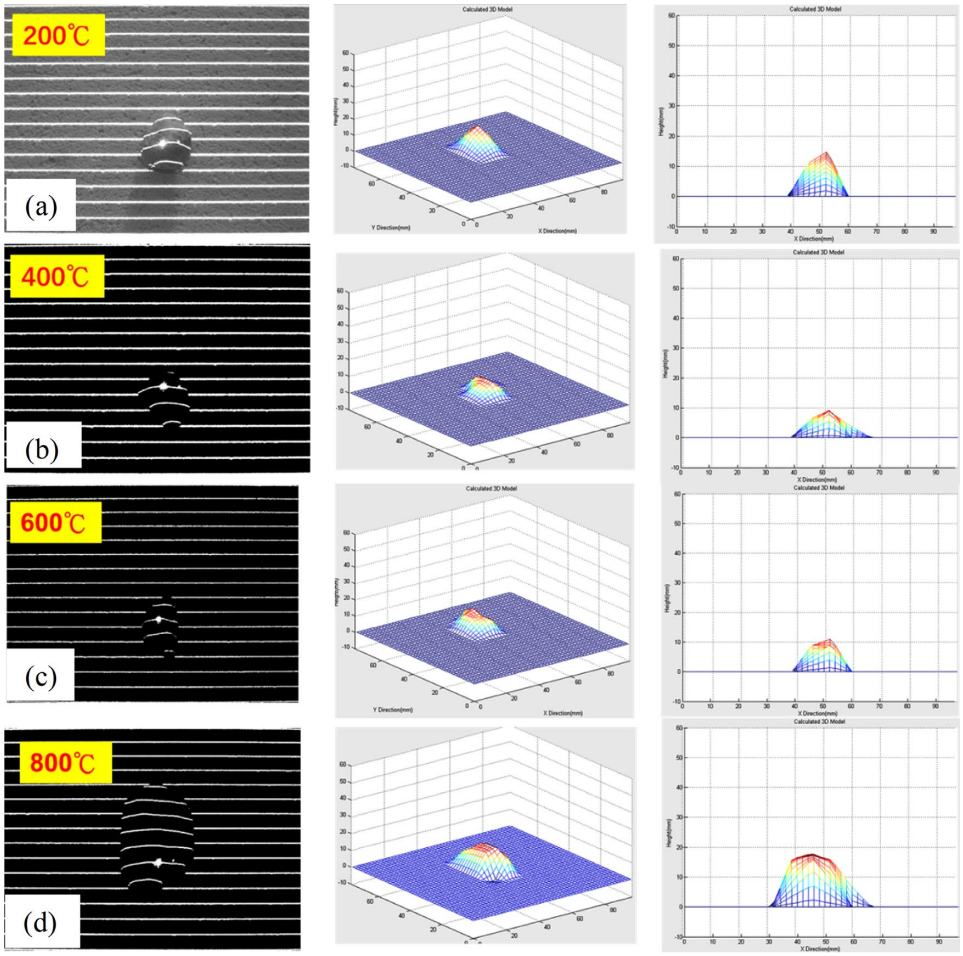

Fig. 10. Reconstructed profile at heated temperature. (a) 200°C. (b) 400°C. (c) 600°C. (d) 800°C. (Online version in color.)

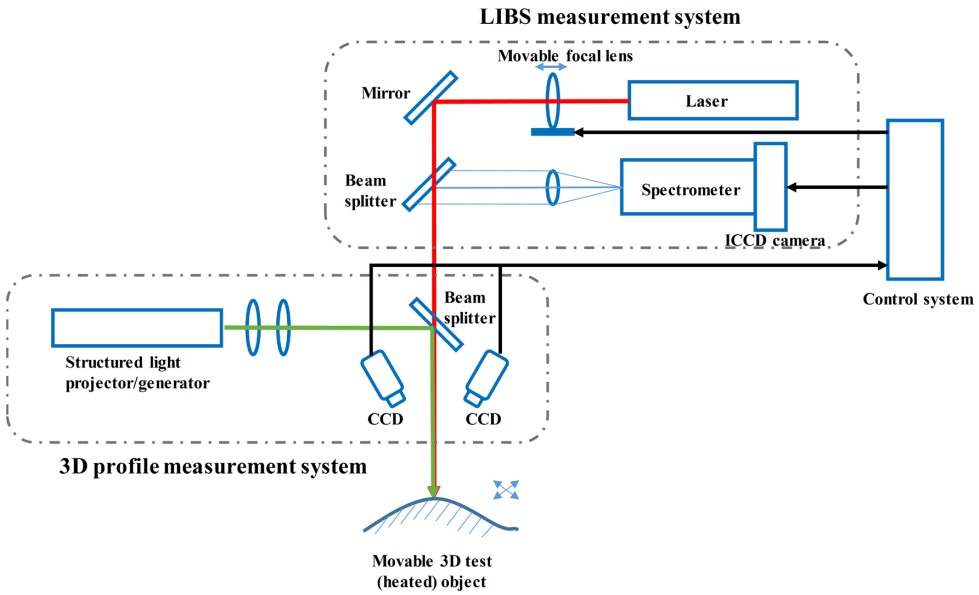

Fig. 11. Proposed innovative co-axial laser beam measurement system of LIBS and 3D profile combination for iron and steel manufacturing processes. (Online version in color.)

coordinate axes was within 2% to evaluate its stability and accuracy of 3D profile measurement system.

According to the above discussion of sample temperature effect, the LIBS signal was affected by the sample temperature. Therefore, the slag sample was also measured under heated temperature conditions for 3D profile measurement. **Figure 10** illustrates the image acquisition at different temperature from 200°C to 800°C. The 3D profile was also influenced by sample temperature. The measured accuracy was evaluated when comparing the results at temperature of 800°C to that at room temperature. The averaged relative error in three coordinate axes was within 10%. The results demonstrated the feasibility of this 3D profile measurement system and its relevant analysis method, even if at high temperature.

According to the above study, the laser beam focus of LIBS is one of the most important factors to be concerned for the LIBS application to industrial processes with the change of a target profile. 3D profile information of the object is required for the positioning of a focused laser beam. Therefore, the combination of LIBS and 3D profile measurement is proposed as an innovative co-axial laser beam measurement system with the autofocus feature, as presented in **Fig. 11**. The laser structured 3D profile measuring system will be applied to detect 3D profile of the movable 3D test object. The acquired profile information will be collected by PC controller. According to the measured profile information of target, the focus point can be automatically and immediately adjusted by the movable focal lens to enhance the detection limit and reliability of measurements. This proposed autofocus LIBS system combined LIBS and 3D profile measurement will promote LIBS online application.

5. Conclusions

The real-time elemental analysis and monitoring of iron and steel manufacturing processes are very important for the improvement of metallurgical techniques and quality of products. Laser-induced breakdown spectroscopy (LIBS) was employed for remote measurement. The remote open-path LIBS measurement was verified using different steel samples. The measurement characteristics at the remote distances of 3.9 m and 1.2 m were discussed in this paper.

(1) The steel sample was measured at different sample temperature. The emission intensity increased when increasing the sample temperature. Therefore, LIBS quantitative analysis should consider the sample temperature influence. The LTD effect and sample angle effect were also discussed under different conditions. When the actual conditions deviated from the designed values, the emission intensity decreased. The results demonstrated the robustness of remote open-path LIBS system. However, the correction is very necessary for online measurement to improve the detection ability of remote open-path LIBS system.

(2) The 3D profile measurement system was also employed to detect the profile information of slag sample at different sample temperature. 3D profile of measured slag was reconstructed using the fringes projection system. It demonstrated the feasibility of 3D profile of measured irregular sample, even if at different sample temperature.

According to the above discussion, an innovative co-axial laser beam measurement system combining LIBS and 3D profile techniques is proposed to automatically adjust the focus unit and measure the sample contents. The further study of this promising method will be developed to online application for real-time elemental analysis and monitoring of iron and steel manufacturing processes.

Acknowledgments

The present work was supported by Research Project I of the Iron and Steel Institute of Japan (Realtime Analysis of Molten Steel, 2017–2019), Collaboration Program between Tokushima University and National Taiwan University of Science and Technology, National Natural Science Foundation of China (No. 51506171).

REFERENCES

1) Z. Z. Wang, Y. Deguchi, F. J. Shiou, J. J. Yan and J. P. Liu: *ISIJ Int.*, **56** (2016), 723.
2) Y. C. Yip, J. C. Lam and W. F. Tong: *TrAC Trends Anal. Chem.*, **28** (2009), 214.
3) M. Aula, T. Demus, T. Echterhof, M. Huttula, H. Pfeifer and T. Fabritius: *ISIJ Int.*, **57** (2017), 478.
4) T. Takayama, R. Murao and M. Kimura: *ISIJ Int.*, **58** (2018), 1069.
5) M. Nagoshi, T. Aoyama, Y. Tanaka, T. Ishida, S. Kinoshiro and K. Kobayashi: *ISIJ Int.*, **53** (2013), 2197.
6) V. K. Karandashev, A. N. Turanov, H. M. Kuß, I. Kumpmann, L. V. Zadnepruk and V. E. Baulin: *Mikrochim. Acta* **130** (1998), 47.
7) H. Kataoka, Y. Okamoto, S. Tsukahara, T. Fujiwara and K. Ito: *Anal. Chim. Acta*, **610** (2008), 179.
8) D. A. Cremers and L. J. Radziemski: Handbook of Laser-Induced Breakdown Spectroscopy, John Wiley & Sons, West Sussex, (2006), 171.
9) R. Noll: Laser-Induced Breakdown Spectroscopy: Fundamentals and Applications, Springer-Verlag, Berlin, Heidelberg, (2012), 229.
10) Y. Deguchi: Industrial Applications of Laser Diagnostics, CRC Press, Taylor & Francis, New York, (2011), 107.
11) Z. Wang, F. Z. Dong and W. D. Zhou: *Plasma Sci. Technol.*, **17** (2015), 617.
12) Z. Z. Wang, Y. Deguchi, Z. Z. Zhang, Z. Wang, X. Y. Zeng and J. J. Yan: *Front. Phys.*, **11** (2016), 114213.
13) Y. T. Fu, Z. Y. Hou, Y. Deguchi and Z. Wang: *Plasma Sci. Technol.*, **21** (2019), 030101.
14) F. Z. Dong, X. L. Chen, Q. Wang, L. X. Sun, H. B. Yu, Y. X. Liang, J. G. Wang, Z. B. Ni, Z. H. Du, Y. W. Ma and J. D. Lu: *Front. Phys.*, **7** (2012), 679.
15) Y. Zhang, Y. H. Jia, J. W. Chen, X. J. Shen, Y. Liu, L. Zhao, D. L. Li, P. C. Han, Z. L. Xiao and H. Q. Ma: *ISIJ Int.*, **54** (2014), 136.
16) J. Gruber, J. Heitz, H. Strasser, D. Bauerle and N. Ramaseder: *Spectrochim. Acta B*, **56** (2001), 685.
17) G. Hubmer, R. Kitzberger and K. Mörwald: *Anal. Bioanal. Chem.*, **385** (2006), 219.
18) L. X. Sun, H. B. Yu, Z. B. Cong, Y. Xin, Y. Li and L. F. Qi: *Spectrochim. Acta B*, **112** (2015), 40.
19) R. Noll, H. Bette, A. Brysch, M. Kraushaar, I. Monch, L. Peter and V. Sturm: *Spectrochim. Acta B*, **56** (2001), 637.
20) S. Palanco, S. Conesa and J. J. Laserna: *J. Anal. At. Spectrom.*, **19** (2004), 462.
21) S. Palanco, J. M. Baena and J. J. Laserna: *Spectrochim. Acta B*, **57** (2002), 591.
22) L. X. Sun, Y. Xin, Z. B. Cong, Y. Li and L. F. Qi: *Adv. Mater. Res.*, **694**–**697** (2013), 1260.
23) F. J. Shiou, H. H. Chen and C. H. Tsai: *J. Chin. Inst. Eng.*, **33** (2010), 141.
24) K. C. Fan and T. H. Tsai: *Robot. Comput. Integr. Manuf.*, **17** (2001), 215.
25) H. C. Nguyen and B. R. Lee: *Int. J. Precis. Eng. Manuf.*, **15** (2014), 415.
26) F. J. Shiou and Y. W. Deng: *Key Eng. Mater.*, **381**–**382** (2008), 233.
27) M. Chang and K. H. Lin: *Opt. Lasers Eng.*, **30** (1998), 503.
28) R. T. Lee and F. J. Shiou: *Measurement*, **44** (2011), 1.
29) M. C. Cui, Y. Deguchi, S. Tanaka, Z. Z. Wang, M. Y. Jeon, Y. Fujita and S. D. Zhao: *Plasma Sci. Technol.*, **21** (2019), 034007.
30) M. C. Cui, Y. Deguchi, Z. Z. Wang, Y. Fujita, R. W. Liu, F. J. Shiou and S. D. Zhao: *Spectrochim. Acta B*, **142** (2018), 14.
31) C. López-Moreno, S. Palanco and J. J. Laserna: *Spectrochim. Acta B*, **60** (2005), 1034.